JPE 18-5-17

https://doi.org/10.6113/JPE.2018.18.5.1479
ISSN(Print): 1598-2092 / ISSN(Online): 2093-4718

Single-Inductor, Multiple-Input-Single-Output Converter Based Energy Mixer for Power Packet Distribution System

C. M. F. S. Reza†, Dylan Dah-Chuan Lu*,**, Ling Qin***, and Jian Qi*

†,*School of Electrical and Information Engineering, The University of Sydney, NSW, Australia
**School of Electrical and Data Engineering, University of Technology Sydney, NSW, Australia
***Department of Electrical Engineering, Nantong University, Nantong, China

Abstract

Power packet (PP) distribution system distributes power to different loads that share the same distribution cable in a packetized form. When compared with conventional power systems, a PP distribution system (PPDS) can reduce standby power, eliminate Point-of-Load (PoL) power conversion, and intelligently control the load demand from the source side. Due to the absence of PoL conversion, when multiple power sources at different voltage levels and conditioning requirements jointly send power to various loads at different voltage ratings, the generated voltage has an irregular shape. A large filter at each of the load sides is required to reduce such a large voltage ripple. In this paper, a single-inductor, multiple-input-single-output converter structure based multiple-energy-source mixer is proposed. It combines PP generation, maximum power point tracking (MPPT) of renewable energy sources (RESs) and filtering at the source side. To demonstrate the possible renewable energy integration, a PV panel is used as a power source together with other constant voltage sources. The PV power is approximately tracked using the constant voltage method and it is used for each of the PP generations. The proposed PP distribution system is experimentally verified and it is shown that a conventional PI controller is sufficient for stable system operation.

Key words: MPPT, Multiple-energy-source mixer, Power packet, Renewable energy

I. Introduction

The utilization of renewable energy sources has increased significantly since it is an effective way to reduce fossil fuel consumption. Nevertheless, the inherent challenges of power generation from RESs include intermittency, uncertainty and complex power management when integrated with existing electricity infrastructures. The employment of the microgrid concept to solve this issue has become popular nowadays. The microgrid concept is applicable to both AC and DC power systems [1]. DC grids offer a more efficient power conversion [2]-[4] when compared to AC grids when RESs are installed locally. This is due to the fact that most RESs, especially in residential areas, for example PV, fuel cell, etc. generate DC power. In DC distribution systems, the extra power dissipation due to conventional DC/AC and AC/DC conversions can be avoided. Therefore, DC distribution is considered in this paper.

Effective power management is essential for microgrids in terms of proper power distribution and system stability [5]. A complex central power management scheme is adopted in smart grid systems to manage the power on the load side [6], [7]. Although a smart automation system is adopted, unpredictable load change behavior affects the power flow management [6], [8]. An energy internet (EI) was recently introduced where energy can be transferred safely in a packeted manner according to certain requirements. While smart grids are focused on the intellectualization and informationization of conventional grids, an EI can be considered as Smart Grid 2.0 [6], [9]. It is capable of sending

Manuscript received Jan. 2, 2018; accepted Apr. 2, 2018
Recommended for publication by Associate Editor Jonghoon Kim.
†Corresponding Author: susan.reza@sydney.edu.au
Tel: +61406401987, The University of Sydney
*School of Electr. and Inform. Eng., The Univ. of Sydney, Australia
**School of Electr. and Data Eng., Univ. of Tech. Sydney, Australia
***Department of Electrical Engineering, Nantong University, China

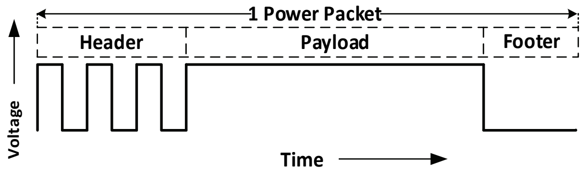

Fig. 1. Power packet structure [17].

packeted energy and delivering it to different addresses depending on the demands of energy routers. It uses the status of sources and loads to choose the best pathway for sending energy packets. It can be a good solution for complex power networks that need to balance power generation and demand [9].

The packetized power scheme implements an approval process that is in place for loads intended to tap onto power lines [10]. This can assure system security and stability. An efficient power flow control can also be ensured using this method [11]. It is not obvious in the PPDS reported in [12]-[15], converting from the input voltages to a standard voltage level, which is one of the main features of PPDS. Hence, eliminating an intermediate voltage conversion stage increases the overall power distribution efficiency. Loads are only connected to a distribution line when it receives the demanded payload. This makes the PPDS less "congested" and safer when compared to existing power distribution systems [6]. A separate communication channel can also be used to transfer the information required for effective payload generation and distribution. Hence, payload generation is very important in power packet distribution system.

Each PP consists of a header and a footer as shown in Fig. 1. They carry information of the power distribution and payload which is the actual load power to be transferred. A PP distribution system (PPDS) includes a mixer and a router. In the PPDS, pulse power is generated from a DC source. An information tag can be attached electrically to the generated voltage waveform. The attached information tag is used to identify and distribute the demanded payload to the requested load. In [16], two different router structures are reported. One can route a power packet to a load directly and another is capable of forwarding the received power packet to another router by attaching an information tag. A modified power packet format is presented in [17], with reduced the footer bit to reduce the transitional switching loss.

A single DC power source is used while generating each payload using the mixer reported in [14], [18]. The DC sources can be obtained from rectified AC voltage sources such as an AC grid, diesel generator or wind turbine generator. To enable the integration of multiple DC sources, for example a mix of conventional and RESs, the PP system should be capable of combining these sources for each PP generation. However, since the sources are likely to be operated at different voltages, the PP generated from mixing these sources will not be smooth or regulated.

A single-inductor multiple-input-single-output buck converter based mixer is proposed to share power from different energy sources. In addition, internal filtering of the converter is used to smooth and regulate the PP voltage. The multi-input buck converter topology reported in [19]-[24] is adopted in this paper for the purpose of developing a mixer for a power packet distribution system. Nevertheless, a modulation scheme that is different from that in [19]-[24] is proposed in this paper. This is mainly due to the mixing and optimizing of DC and renewable energy sources and output power packet generation. A switching scheme is reported in [22] for multi-input converters. This scheme is presented to eliminate the requirement of having the unequal input voltage sources of multi-input converters. The effective duty cycles of switches are an integer multiple of a common duty ratio (CDR) generated by frequency division at a higher frequency [22]. Hence, it allows a single PI controller to control the output voltage utilizing a CDR as the only control variable [22]. A closed loop dual–input buck converter was modeled and analyzed in [23] to propose a novel approach for a close loop regulator design to achieve proper power management of multi-input converters. A systematic theoretical circuitry analysis of an input capacitor added multi input buck converter is carried out in [24], which derived a series of generalize equations to describe the electrical behaviors and characteristics of circuits considering the equivalent series resistance of the input sources of multi-input converters. However, in these papers, fixed DC sources are used as power sources. It should also be noted that the buck converters in [19]-[24] are used for variable continuous output voltage and fixed output voltage. We extended the usage of the multi-input buck converter to condition renewable energy sources and generate power packets, namely, pulsating and variable output voltage pulses.

The idea of mixing power sources is introduced in [25]. This paper extends this idea by conducting a stability analysis of the mixer to confirm the stable operation of the mixer where the mixer is able to smoothly integrate multiple energy sources and operate stably under different conditions, such as PV shading and load demand changes.

In the system proposed in this paper, preferences can be given to specific RESs. In an experiment, a PV panel and another power source are mixed and used while in [14], [18] only ideal DC power supplies are considered. This paper demonstrates that MPPT and power mixing can be achieved simultaneously. To simplify the system design and sufficiently demonstrate the system operation, this paper adopts an approximate voltage MPPT method. However, an accurate MPPT method is also achievable using this system. In this paper, each payload is predefined and distributed alternately. Since the focus of the paper is on power mixing and distribution processes, the information tag is omitted.

This paper is organized as follows. The mixer configuration

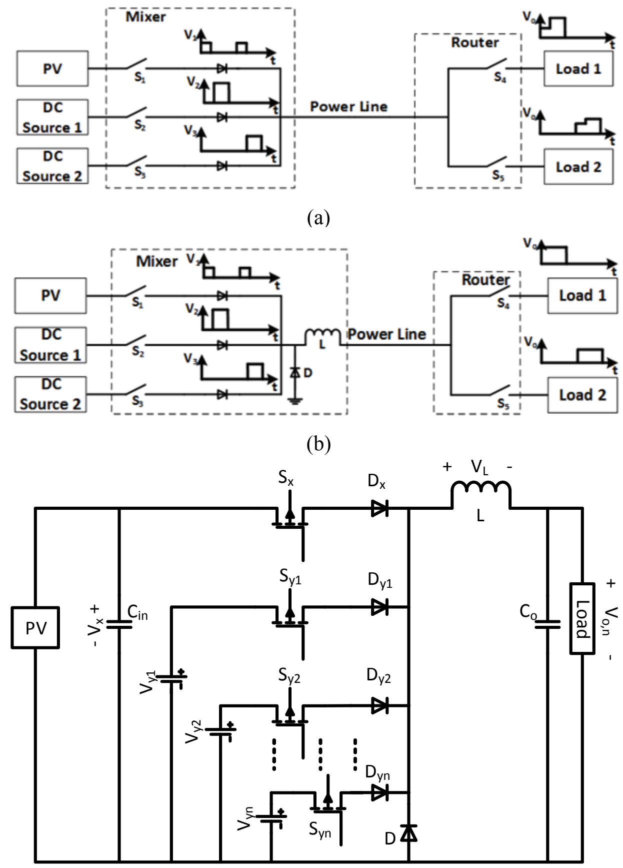

Fig. 2. Power packet distribution system: (a) Mixer presented in [14], (b) Proposed mixer, (c) Proposed mixer circuit diagram.

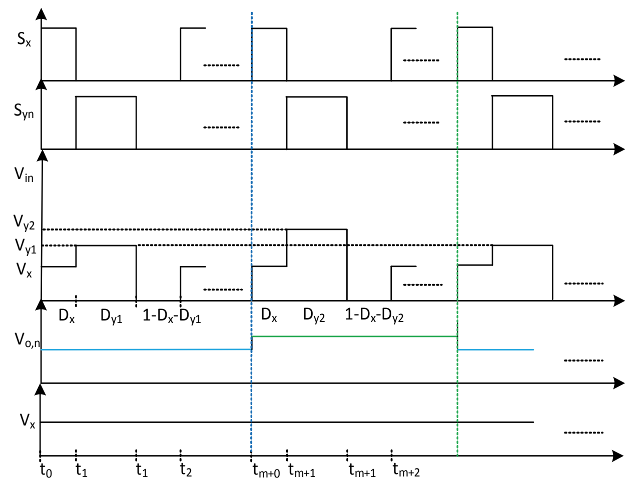

Fig. 3. Schematic of power packet generation waveforms.

is described briefly in Section II. In Section III, the proposed mixer operation principle for PP generation is presented. A stability analysis is discussed in Section IV. Experimental verifications of the proposed mixer are given in Section V. Finally, some conclusions are given in Section VI.

II. Mixer Configuration

A PPDS consists of a mixer and a router. The mixer generates PPs according to the load demand, whereas the router distributes them to the designated loads. The routing information can be transferred through a separate communication cable or by attaching it electronically with the payload which is the actual power supplied to loads. Since, the load power is distributed in a packetized manner, time division multiplexing (TDM) is applied to avoid the payload overlapping. Using the mixer reported in [14], each PP can only be generated through a single source at a particular voltage level to match the load voltage as shown in Fig. 2(a). Hence, multiple voltage sources at distinct voltages cannot simultaneously generate a PP at a single voltage level. To solve this problem a mixer is proposed and shown in Fig. 2(b).

The proposed mixer has power sharing capability between multiple sources and can generate PPs at distinct voltage levels to fulfill load demands which are smooth and regulated. Another good feature of the proposed mixer is that it can prioritize the RESs for power sharing in every PP generation which can maximize RES utilization. A circuit diagram of the proposed mixer is shown in Fig. 2(c). Internal filtering functionality enables the proposed mixer to generate PPs at different voltage levels.

III. Proposed Mixer Operation Principle

The proposed mixer operation principle, which utilizes available energy sources for power packets generation at distinct voltage levels, is explained below. The MPP voltage of a PV module is V_x. Each voltage source (V_{y1} to V_{yn}) can contribute power alongside the PV while generating PPs at distinct voltage levels as shown in Fig. 3. In the analysis, it has been considered that V_{yn} shares power with V_x, while generating PPs at the voltage level $V_{o,n}$ according to the following equation by changing the duty cycle.

$$V_{o,n} = d_x V_x + d_{yn} V_{yn} \tag{1}$$

The controller maintain the voltages V_x and $V_{o,n}$ by adjusting d_x and d_{yn}, respectively. In each switching cycle, three different switching modes appear as follows:

A. Switching Mode 1(d_x)

In this mode, the switch S_x is turned on while switch S_{yn} is turned off to supply energy from the PV. The mixer equivalent circuit in this mode is shown in Fig. 4(a). The corresponding equations for Switching Mode 1 are as follows.

$$\left.\begin{aligned} C_{in}\frac{dv_x}{dt} &= i_{pv} - i_L \\ C_o\frac{dv_{o,n}}{dt} &= i_L - \frac{v_{o,n}}{R} \\ L\frac{di_L}{dt} &= v_x - v_{o,n} \end{aligned}\right\} \tag{2}$$

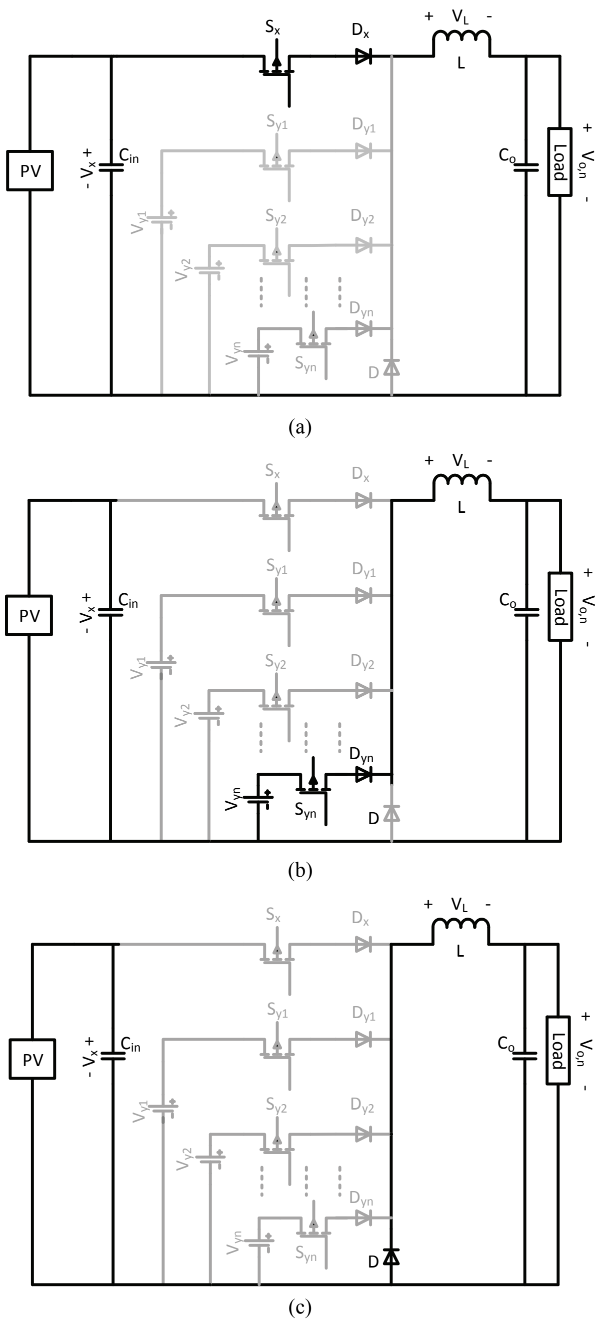

Fig. 4. Power packet generation equivalent circuit during one cycle: (b) Switching mode 1, (c) Switching mode 2, (d) Switching mode 3.

B. Switching Mode 2 (d_{yn})

In this mode, the switch S_{yn} is turned on while the switch S_x is turned off. $V_{y,n}$ supplies energy to the inductor. The mixer equivalent circuit in this state is shown in Fig. 4(b). The equations associated with this mode are given in (3).

$$\left.\begin{aligned} C_{in}\frac{dv_x}{dt} &= i_{pv} \\ C_o\frac{dv_{o,n}}{dt} &= i_L - \frac{v_{o,n}}{R} \\ L\frac{di_L}{dt} &= v_{yn} - v_{o,n} \end{aligned}\right\} \tag{3}$$

C. Switching Mode 3($1 - d_x - d_{yn}$)

In this state, the switches S_x and S_{yn} are turned off. An equivalent circuit of the mixer in this state is shown in Fig. 4(c). In this state, inductor L dispatches its stored energy. The corresponding equations for Switching Mode 3 are given in (4).

$$\left.\begin{aligned} C_{in}\frac{dv_x}{dt} &= i_{pv} \\ C_o\frac{dv_{o,n}}{dt} &= i_L - \frac{v_{o,n}}{R} \\ L\frac{di_L}{dt} &= -v_{o,n} \end{aligned}\right\} \tag{4}$$

IV. Stability Analysis of the Mixer

Small-signal modeling is an important method to analyze the dynamic behavior of the proposed mixer. To properly design and analyze the stability of the controller, it is necessary to extract a dynamic model of the mixer around the designated operating point. The proposed payload generator is controlled by the switches S_x and S_{yn}, while generating PPs at the voltage $V_{o,n}$. By adjusting the duty cycle of S_x, the voltage across the PV can be adjusted. On the other hand, payload voltage levels can be generated by adjusting the duty cycle of S_{y1} to S_{yn}. S_x controls the PV voltage and helps achieve the payloads of different voltage levels by working with S_{y1} to S_{yn} depending on the load demand. For each power packet generation, two control variables hence two controllers are required. One is to control the PV voltage and the other is to control the output voltage. Each of the PPs can be generated by sharing power from the PV with other power sources. In the proposed design, preferences are given to the PV to share power in each of the PP generations to maximize renewable energy intake. According to small signal modeling, the input voltage, state variables and duty ratios have two parts. The two parts are perturbations and dc values. Hence, for the proposed power packet generation system (5) is obtained. A dynamic model of the mixer while generating a payload is derived as below:

$$\left.\begin{aligned} v_x(t) &= v_x^{\bullet}(t) + V_x \\ v_{yn}(t) &= v_{yn}^{\bullet}(t) + V_{yn} \\ v_{o,n}(t) &= v_{o,n}^{\bullet}(t) + V_{o,n} \\ i_{pv}(t) &= i_{pv}^{\bullet}(t) + I_{pv} \\ i_L(t) &= i_L^{\bullet}(t) + I_L \\ d_x(t) &= d_x^{\bullet}(t) + d_{xs} \\ d_{yn}(t) &= d_{yn}^{\bullet}(t) + d_{yns} \end{aligned}\right\} \tag{5}$$

For the controller design, the capacitor voltage across the PV $v_x(t)$ along with the output capacitor voltage $v_{o,n}(t)$ and inductor current $i_L(t)$ are state variables. Applying averaging to (2)-(4) and multiplying them by their corresponding effective duty cycles, equation (6) can be obtained.

$$\left.\begin{aligned} C_{in}\frac{dv_x}{dt} &= [d_x + (1-d_x-d_{yn}) + d_{yn}]i_{pv} - d_x i_L \\ C_o\frac{dv_{o,n}}{dt} &= i_L - \frac{v_{o,n}}{R} \\ L\frac{di_L}{dt} &= d_x v_x - d_x v_{o,n} + d_{yn}v_{yn} - d_{yn}v_{o,n} \\ &\quad -(1-d_x-d_{yn})v_{o,n} \end{aligned}\right\} \quad (6)$$

Substituting (5) into (6) yields (7).

$$\left.\begin{aligned} C_{in}\frac{dv_x^{\bullet}}{dt} &= I_{pv} + i_{pv}^{\bullet}(t) - d_{xs}i_L^{\bullet}(t) - d_x^{\bullet}(t)I_L \\ &\quad -d_x^{\bullet}(t)i_L^{\bullet}(t) - d_{xs}I_L \\ C_o\frac{dv_{o,n}^{\bullet}}{dt} &= i_L^{\bullet}(t) + I_L - \frac{v_{o,n}^{\bullet}(t)}{R} - \frac{V_{o,n}}{R} \\ L\frac{di_L^{\bullet}}{dt} &= d_{xs}V_x + d_{xs}v_x^{\bullet}(t) + V_x d_x^{\bullet}(t) + d_x^{\bullet}(t)v_x^{\bullet}(t) \\ &\quad +d_{yns}V_{yn} + d_{yns}v_{yn}^{\bullet}(t) + V_{yn}d_{yn}^{\bullet}(t) \\ &\quad +d_{yn}^{\bullet}(t)v_{yn}^{\bullet}(t) - v_{o,n}^{\bullet}(t) - V_{o,n} \end{aligned}\right\} \quad (7)$$

Ignoring the second order term and considering $v_{yn}^{\bullet}(t)= 0$, (8) can be obtained from (7).

$$\left.\begin{aligned} C_{in}\frac{dv_x^{\bullet}}{dt} &= I_{pv} + i_{pv}^{\bullet}(t) - d_{xs}i_L^{\bullet}(t) - d_x^{\bullet}(t)I_L - d_{xs}I_L \\ C_o\frac{dv_{o,n}^{\bullet}}{dt} &= i_L^{\bullet}(t) + I_L - \frac{v_{o,n}^{\bullet}(t)}{R} - \frac{V_{o,n}}{R} \\ L\frac{di_L^{\bullet}}{dt} &= d_{xs}V_x + d_{xs}v_x^{\bullet}(t) + V_x d_x^{\bullet}(t) + d_{yns}V_{yn} \\ &\quad +V_{yn}d_{yn}^{\bullet}(t) - v_{o,n}^{\bullet}(t) - V_{o,n} \end{aligned}\right\} \quad (8)$$

From (8), dc and small signal models can be found which are shown in (9) and (10), respectively.

$$\left.\begin{aligned} 0 &= I_{pv} - d_{xs}I_L \\ 0 &= I_L - \frac{V_{o,n}}{R} \\ 0 &= d_{xs}V_x + d_{yns}V_{yn} - V_{o,n} \end{aligned}\right\} \quad (9)$$

$$\left.\begin{aligned} C_{in}\frac{dv_x^{\bullet}}{dt} &= i_{pv}^{\bullet}(t) - d_{xs}i_L^{\bullet}(t) - d_x^{\bullet}(t)I_L \\ C_o\frac{dv_{o,n}^{\bullet}}{dt} &= i_L^{\bullet}(t) - \frac{v_{o,n}^{\bullet}(t)}{R} \\ L\frac{di_L^{\bullet}}{dt} &= d_{xs}v_x^{\bullet}(t) + V_x d_x^{\bullet}(t) + V_{yn}d_{yn}^{\bullet}(t) - v_{o,n}^{\bullet}(t) \end{aligned}\right\} \quad (10)$$

In the proposed control scheme, $d_{xs} + d_{yns} \leq 1$. From (9), the following relation can be obtained.

$$V_{o,n} = d_{xs}V_x + d_{yns}V_{yn} \quad (11)$$

From (11) it can be observed that $V_{o,n} \epsilon [0, \max(V_x, V_{yn})]$. From this relationship it can be seen that the demanded output voltage level can be varied from zero to the maximum of the supply voltage. A power packet having a voltage rating within this limit can be demanded in this proposed structure. Eqn. (10) is in the time domain. Transferring this to the s-domain yields (12).

$$\left.\begin{aligned} sC_{in}v_x^{\bullet}(s) &= i_{pv}^{\bullet}(s) - d_{xs}i_L^{\bullet}(s) - d_x^{\bullet}(s)I_L \\ sC_o v_{o,n}^{\bullet}(s) &= i_L^{\bullet}(s) - \frac{v_{o,n}^{\bullet}(t)}{R} \\ sLi_L^{\bullet}(s) &= d_{xs}v_x^{\bullet}(s) + V_x d_x^{\bullet}(s) + V_{yn}d_{yn}^{\bullet}(s) - v_{o,n}^{\bullet}(s) \end{aligned}\right\} \quad (12)$$

From (12), Eqns. (13) and (14) can be obtained.

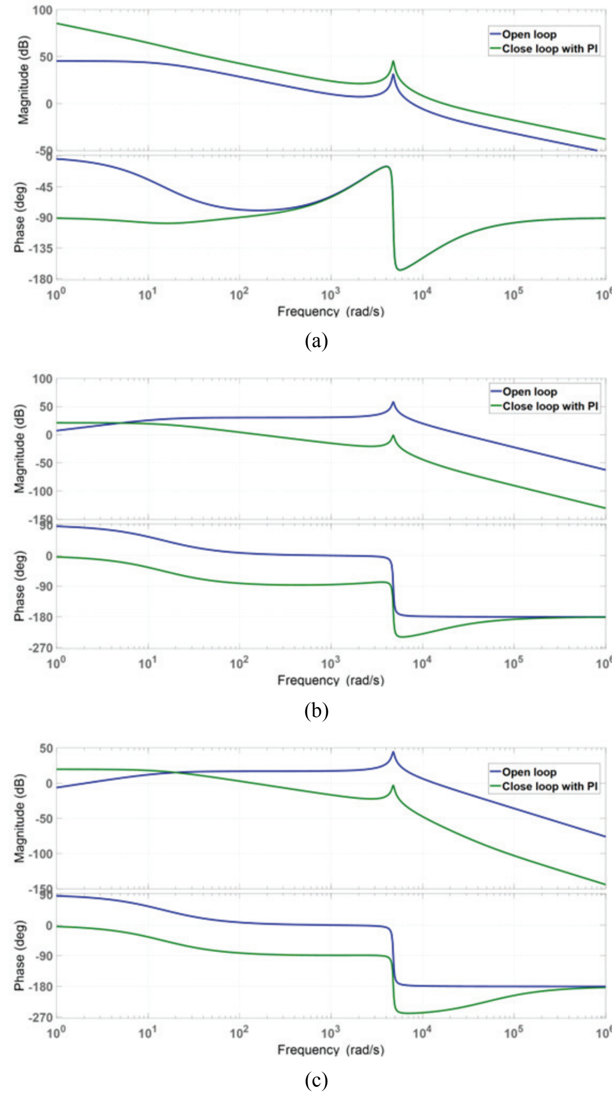

Fig. 5. Bode plots: (a) Bode plots of $F_{ux} * F_m * G_x(s)$, (b) Bode plots of $F_{u2} * F_m * G_{y2}(s)$, (c) Bode plots of $F_{u1} * F_m * G_{y1}(s)$.

$$\left.\begin{aligned} G_x(s) &= \left.\frac{v_x^{\bullet}(s)}{d_x^{\bullet}(s)}\right|_{\substack{i_{pv}^{\bullet}(s)=0 \\ d_{yn}^{\bullet}(s)=0}} \\ &= -\frac{s^2LRC_oI_L + s(I_LL + Rd_{xs}V_xC_o) + RI_L + d_{xs}V_x}{s^3LRC_oC_{in} + s^2LC_{in} + s(RC_{in} + RC_od_{xs}^2) + d_{xs}^2} \end{aligned}\right\} \quad (13)$$

$$\left.\begin{aligned} G_{yn}(s) &= \left.\frac{v_{o,n}^{\bullet}(s)}{d_{yn}^{\bullet}(s)}\right|_{\substack{i_{pv}^{\bullet}(s)=0 \\ d_x^{\bullet}(s)=0}} \\ &= \frac{sRC_{in}V_{yn}}{s^3LRC_oC_{in} + s^2LC_{in} + s(RC_{in} + RC_od_{xs}^2) + d_{xs}^2} \end{aligned}\right\} \quad (14)$$

In this design, the voltage levels of the DC power supplies are used as V_{y1}=15V and V_{y2}= 36V, which are used to generate PPs at the two different voltages of $V_{o,1}$=12V and $V_{o,2}$=24V, respectively. A bode diagram of the transfer functions of the system obtained in (13) and (14) are shown in Figs. 5(a), 5(b) and 5(c). From these figures it can be seen

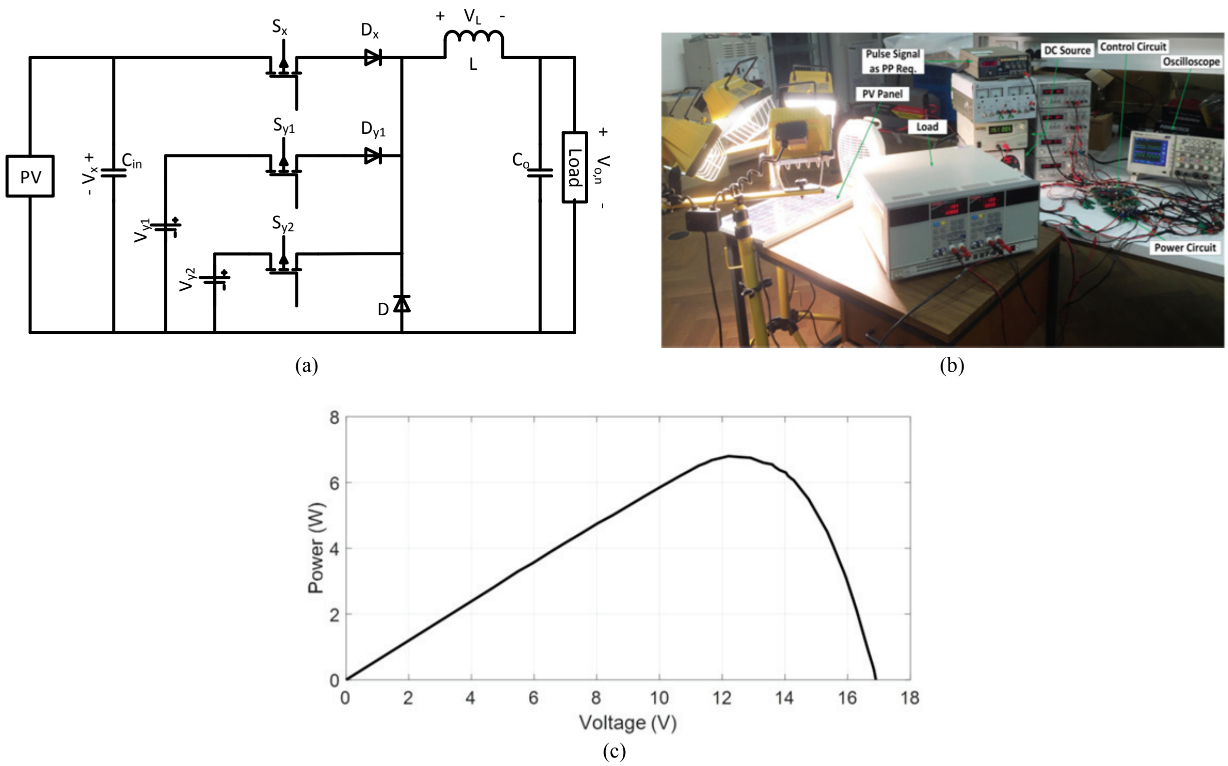

Fig. 6. Hardware setup and P-V curve of the solar panel: (a) Mixer circuit diagram used in the experiment, (b) Hardware setup, (c) P-V curve of the solar panel used in the experiment.

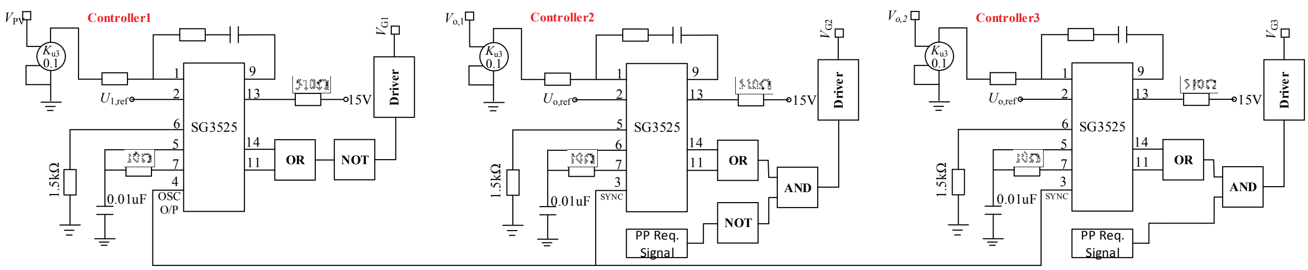

Fig. 7. Control circuit schematic (Controller1 sends a PWM signal to S_x to control the voltage across the PV, Controller2 sends a PWM signal to S_{y1} while generating $V_{o,1}$ power packet, and Controller3 sends a PWM signal to S_{y2} while generating $V_{o,2}$ power packet).

that the systems are stable using PI close loop controllers with $K_{px} = 5$, $K_{py1} = K_{py2} = 0.0004$, and $K_{ix} = 100$, $K_{iy1} = 20$, $K_{iy2} = 5$ where the phase margins are 49.2, 95.7 and 96.1 degrees. The scaled feedback voltages $F_{ux} = k_u V_x$, $F_{u1} = k_u V_{o,1}$ and $F_{u2} = k_u V_{o,2}$ are used where the scaling factor $k_u = 0.1$ is being used. The PWM modulator gain of the IC is $F_m = 0.4$.

V. Experimental Verifications

To verify the proposed mixer and controller, a laboratory prototype having three inputs, as shown in Fig. 6(a), is built and shown in Fig. 6(b). The following circuit parameters are used: V_x = MPP voltage of the PV panel (12V), V_{y1} = 15V, V_{y2} = 36V, C_{pv} = 470μF, L = 0.1mH, R = 10Ω, $F_{ux} = F_{u1}$ = 1.2 and F_{u2} = 2.4. Inductor (L) can be chosen according to the requirements discussed in the appendix. A P-V characteristic curve of the solar panel used in the experiment is shown in Fig. 6(c). In the experiment, PPs with voltage ratings of 12V and 24V are generated. It is assumed that the load requests alternate the power packets at two different voltage rating. Hence, in the experiment, a pulsating signal is used to mimic a power packet request signal between the two voltages alternatively. In this experiment, a single load is used to receive both 24V and 12V PP. This is done to simplify the receiving end by omitting the router function and focusing on the proposed mixer performance. The control circuit is shown in Fig. 7.

To implement the PV voltage and power packet voltage regulation a PWM generation controller IC-SG3525 is utilized. Halogen lamps are used to artificially illuminate the PV module which can be seen in Fig. 6(b). It can be clearly seen

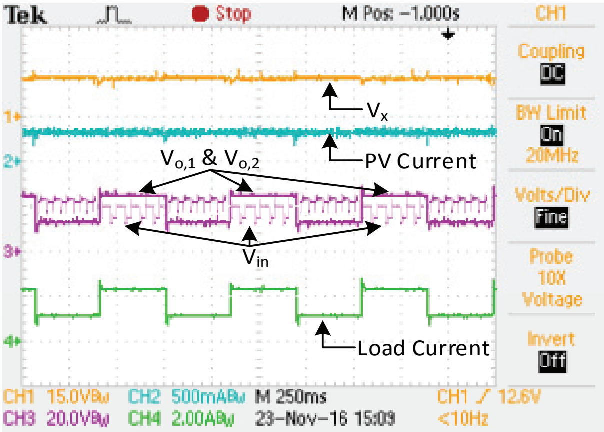

(a)

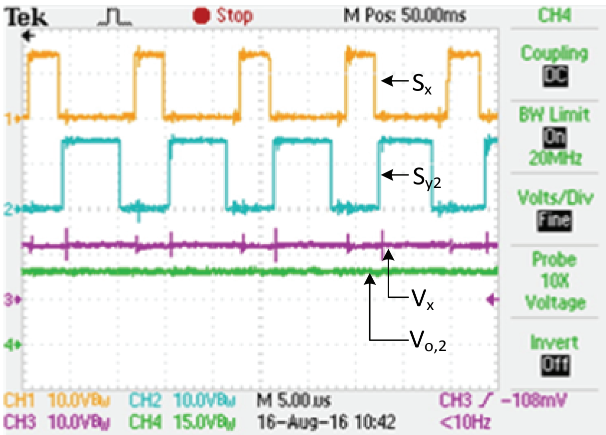

(b)

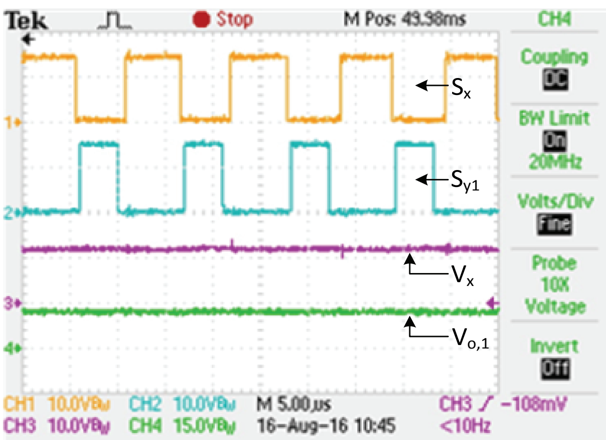

(c)

Fig. 8. Power packet generation: (a) PP generation with 12V and 24V ratings, (b) Switching signal during 24V PP generation, (c) Switching signal during 12V PP generation.

from Fig. 6(c) that the MPP voltage is almost 12 V. To control the PV voltage, an approximate MPPT technique is used, which utilizes a PI controller. A switching frequency of 90kHz is used in the experiment. The PV shares power in every PP generation as long as the PV voltage and output voltage conditions are satisfied. Therefore, power is shared from any voltage sources and the PV while generating every PP.

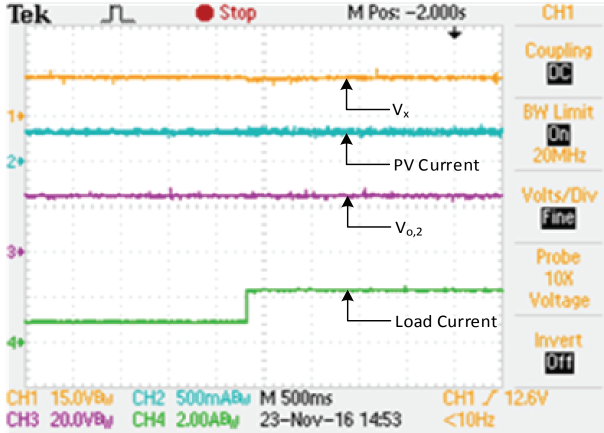

(a)

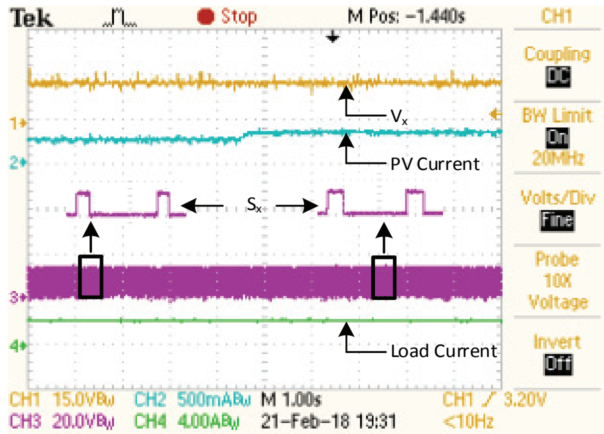

(b)

Fig. 9. Effect of change in load demand and PV generation: (a) 24V PP generation while changing the load demand, (b) 24V PP generation during PV shading.

It can be seen from Fig. 8(a) that PPs at 12V and 24V are alternately generated as shown in CH3. Two different load currents are shown in CH4 during PPs generation at two distinct voltage levels. The PV voltage is maintained at 12V to attain approximate MPPT and a constant PV current is shown in CH1 and CH2, respectively in Fig. 8(a). The voltage shape is irregular before filtering, while a smooth output voltage is generated because of the internal filtering of the proposed mixer.

The switching signal S_x and S_{y2} are shown in CH1 and CH2 in Fig. 8(b). S_x is used to control the PV voltage and S_{y2} is used in 24V power packet generation. A smooth 24V power packet is generated as shown in CH4, while the PV voltage is maintained at 12V which can be seen from CH3 in Fig. 8(b). Similarly, a constant 12V power packet is generated by controlling the switch S_{y1} while the PV voltage is maintained at a desired level by controlling S_x. From Fig. 8(b) and 8(c), it can be seen that the duty cycle d_x is larger while generating a 12V power packet than it is while generating a 24V PP. The PV voltage needs to be maintained at a desired level and at the same time the output voltage equation presented in (1) needed to be satisfied.

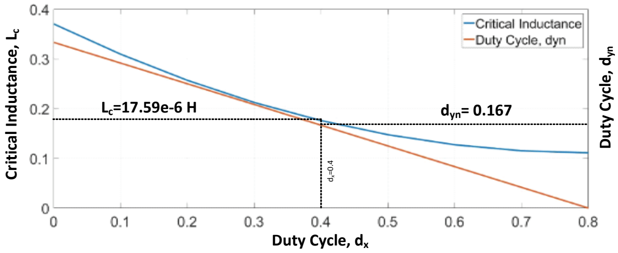

Fig. 10. Critical inductance for different duty cycle combinations.

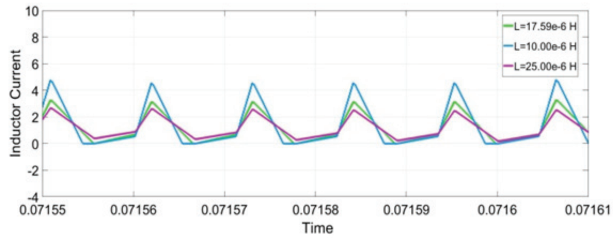

Fig. 11. Inductor currents for different inductors.

Fig. 9(a) shows the mixer performance during a change in the load demand when generating a 24V PP. Initially, the load resistance is 20Ω. Afterwards, a 15Ω resistor is added in parallel with the load. From CH1 and CH3 of Fig. 9(a) it can be seen that the voltage across the PV and the load voltage are maintained at desired levels even though the load current is changed as shown in CH4. The PV current, as shown in CH2, is kept constant during the transient response. This is due to fact that the difference between the PV current and load current is supplied by the voltage source V_{y2} while the PV and voltage source V_{y2} share power while generating a 24V power packet. This is an inherent feature of the converter operating in the CCM which automatically adjusts the current [26].

Finally, the mixer performance during the PV partial shading condition is validated as shown in Fig. 9(b), while generating a 24V power packet. A fixed load R = 10Ω is used in this case. Partial shading is applied over the PV panel to check that it can maintain the MPP while satisfying the load demand by sharing power with other sources. CH1 and CH2 of Fig. 9(b) depict the voltage across the PV and PV current. It can be seen that there is a change in the switching signal of the switch S_1, which is shown in CH3. The load current remains constant as shown in CH4 (Fig. 9(b)).

VI. CONCLUSIONS

A single-inductor multiple-input-single-output converter based mixer is proposed for power packet distribution system. The power mixing capability of the proposed mixer allows for the generation of PPs by sharing the power from more than a single source. The proposed control scheme is designed in such a way that the PVs can get preference to share power while generating PPs. The stability of the mixer is analyzed to demonstrate the power mixing feature of the proposed mixer while power conditioning and voltage regulation are maintained simultaneously. A hardware prototype with a close loop system is analyzed and the PP voltages are controlled by a PI controller. In addition, the PV voltage is regulated using a PI controller by adopting an approximate MPPT technique which is experimentally verified for the proposed mixer. Preference can be given to renewable power sources that can maximize renewable energy utilization. The internal filtering capability of the proposed mixer can generate smooth and regulated PPs at a desired voltage level. While generating PPs, the controller can adjust the duty cycles when there is a change in the load demand or PV shading. Any number of power sources at different voltage levels can be utilized to generate PPs at different voltage ratings. In addition, the controller can be designed using the small signal model derived in this paper. The proposed mixer structure for PP generation can be applied in many areas such as electric vehicles, smart home power management and microgrids.

APPENDIX

The inductor can be chosen using an equation reported in [21]. For two inputs mixer critical inductance, (L_c) can be calculated using equation (A1).

$$L_c = \frac{R}{2f}\left[(-d_x^2 + 2d_x)\left(\frac{V_x}{V_{o,n}}\right) + \left(d_x^2 - (d_x + d_y)^2 + 2d_{yn}\right)\left(\frac{V_{yn}}{V_{o,n}}\right) - 1\right] \quad \text{(A1)}$$

where R and f are the load resistance and switching frequency, respectively.

Assuming $V_{o,n}$=12V, V_x=15V and V_{yn}=36V, equation (A2) can be found from (1).

$$15d_x + 36d_{yn} = 12 \;\; For \;\; \left.\begin{matrix} 0 \le d_x \le 0.8 \\ 0 \le d_{yn} \le 0.33 \end{matrix}\right\} \quad \text{(A2)}$$

For different combinations of d_x and d_{yn}, L_c is different as can be seen from Fig. 10. To show a properly critical inductance and duty cycle at the same scale, the critical inductance is multiplied by a scaling factor of 10^4. For example, when d_x=0.4 and d_{yn}=0.167, then for R=10Ω and f=90kHz, the critical inductance L_c can be found using (A1), which is 17.59μH. The inductor currents for different values are shown in Fig.11. It can be seen that the mixer is in the CCM mode when the inductor value is higher then L_c and that it is in the DCM mode when the inductor value is lower then L_c.

ACKNOWLEDGMENT

The authors would like to thank the financial support provided by the University of Sydney RTP scholarship for this research work.

REFERENCES

[1] X. Wang, J. M. Guerrero, F. Blaabjerg, and Z. Chen, "A review of power electronics based microgrids," *J. Power Electron.,* Vol. 12, No. 1, pp.181-192, Jan. 2012.

[2] D. D.-C. Lu and V. G. Agelidis, "Photovoltaic-battery-powered dc bus system for common portable electronic devices," *IEEE Trans. Power Electron.*, Vol. 24, No. 3, pp 849-855, Feb. 2009.

[3] S. Singh, V. Kumar, and D. Fulwani, "Mitigation of destabilising effect of CPLs in island DC micro-grid using non-linear control," *IET Power Electron.,* Vol. 10, No. 3, pp. 387-397, Mar. 2017.

[4] C. Liu, D. Zhu, J. Zhang, H. Liu, and G. Cai, "A bidirectional dual buck-boost voltage balancer with direct coupling based on a burst-mode control scheme for low-voltage bipolar-type DC microgrids," *J. Power Electron.,* Vol. 15, No. 6, pp. 1609-1618, Nov. 2015

[5] G. Wang, V. Kekatos, A. J. Conejo, and G. B. Giannakis, "Ergodic energy management leveraging resource variability in distribution grids" *IEEE Trans. Power Syst.*, Vol. 31, No. 6, pp. 4765-4775, Nov. 2016.

[6] C. M. F. S. Reza and D. D.-C. Lu, "Design and implementation of a packeted DC power system using a modified power packet structure," *IET Power Electron.,* Vol. 11, No. 9, pp. 1603-1610, Aug 2018.

[7] M. Erol-Kantarci and H. T. Mouftah, "Wireless sensor networks for cost-efficient residential energy management in the smart grid," *IEEE Trans. Smart Grid*, Vol. 2, No. 2, pp 314-325, Jun. 2011.

[8] R. Abe, H. Taoka, and D. McQuilkin, "Digital grid: Communicative electrical grids of the future," *IEEE Trans. Smart Grid*, Vol. 2, No. 2, pp 399-410, Jun. 2011.

[9] J. Cao and M. Yang, "Energy internet–towards smart grid 2.0," in *Fourth International Conference on Networking and Distributed Computing, IEEE*, pp. 105-110, 2013.

[10] H. Grebel and R. Rojas-Cessa, "Packeted energy delivery system and methods," U.S. Patent US9577428 B2, Feb 21, 2017.

[11] X. Fang, S. Misra, G. Xue, and D. Yang, "Smart grid - the new and improved power grid: A survey," *IEEE Commun. Surveys Tuts.,* Vol. 14, No. 4, pp 944-980, Dec. 2012.

[12] T.Takuno, M. Koyama, and T. Hikihara, "In-home power distribution systems by circuit switching and power packet dispatching," in *First International Conference on Smart Grid Communications (Smart Grid Comm), IEEE*, pp. 427-430, 2010.

[13] V. Krylov, D. Ponomarev, and A. Loskutov, "Toward the power intergrid," in *International Energy Conference and Exhibition (EnergyCon), IEEE*, pp. 351-356, 2010.

[14] R. Takahashi, S.-I. Azuma, and T. Hikihara, "Power regulation with predictive dynamic quantizer in power packet dispatching system," *IEEE Trans. Ind. Electron.,* Vol. 63, No. 12, pp 7653-7661, Jul. 2016.

[15] K. Tashiro, R. Takahashi, and T. Hikihara, "Feasibility of power packet dispatching at in-home dc distribution network," in *Third International Conference on Smart Grid Communications (Smart Grid Comm), IEEE*, pp. 401-405, 2012.

[16] R. Takahashi, K. Tashiro, and T.Hikihara, "Router for power packet distribution network: Design and experimental verification," *IEEE Trans. Smart Grid*, Vol. 6, No. 2, pp. 618-626, Jan. 2015.

[17] C. M. F. S. Reza and D. D.-C. Lu, "Improved power routing algorithm for power packet distribution system," *in 5th Global Conference on Consumer Electronics (GCCE), IEEE,* pp. 343-344, 2016.

[18] R. Takahashi, S.-I. Azuma, K. Tashiro, and T. Hikihara, "Design and experimental verification of power packet generation system for power packet dispatching system," *in American Control Conference (ACC), IEEE*, pp. 4368-4373, 2013.

[19] M. Rodríguez, P. Fernández-Miaja, A. Rodríguez, and J. Sebastián, "A multiple-input digitally controlled buck converter for envelope tracking applications in radiofrequency power amplifiers," *IEEE Trans. Power Electron.,* Vol. 25, No. 2, pp 369-381, Aug. 2010.

[20] Y. Li, X. Ruan, D. Yang, F. Liu, and C. K. Tse, "Synthesis of multiple-input DC/DC converters," *IEEE Trans. Power Electron.*, Vol. 25, No. 9, pp 2372-2385, Apr. 2010.

[21] E. Babaei, K. Varesi, and N. Vosoughi, "Calculation of critical inductance in n-input buck dc-dc converter," *IET Power Electron.*, Vol. 9, No. 12, pp. 2434-2444, Oct. 2016.

[22] C. N. Onwuchekwa and A. Kwasinski, "A modified-time-sharing switching technique for multiple-input DC–DC converters," *IEEE Trans. Power Electron.,* Vol. 27, No. 11, pp. 4492-4502, Dec. 2012.

[23] Y. Li, X. Ruan, D. Yang, and F. Liu, "Modeling, analysis and design for hybrid power systems with dual-input DC/DC converter," in *Energy Conversion Congress and Exposition (ECCE), IEEE*, pp. 3203-3210, 2009.

[24] L. Xian, G. Wang, and Y. Wang, "Circuitry and analysis of input-capacitor-added multiple-input buck converters," *IET Power Electron.*, Vol. 6, No. 7, pp. 1415-1426, Sep. 2013.

[25] C. M. F. S. Reza, D. D.-C. Lu, and L. Qin, "Single-inductor multiple-source mixer for DC power packet dispatching system," in *Second International Conference on DC Microgrids (ICDCM), IEEE*, pp. 553-557, 2017.

[26] D. D.-C. Lu, "High voltage stress in single-phase single-stage PFC converters: Analysis and an alternative solution," *IEEE Trans. Ind. Electron.*, Vol. 63, No. 1, pp 133-143, Jan. 2016.

C. M. F. S. Reza received his B.S. degree in Electrical and Electronic Engineering from the Chittagong University of Engineering and Technology (CUET), Pahartali, Bangladesh, in 2010; and his M.S. degree in Electrical Engineering from the University of Malaya, Kuala Lumpur, Malaysia, in 2014. He is presently working towards his Ph.D. degree in Electrical and Information Engineering at the University of Sydney, Sydney, Australia. From November 2011 to October 2014, he was a Research Assistant at the Power Electronics and Renewable Energy Research Laboratory (PEARL), University of Malaya, Kuala Lumpur, Malaysia. His current research interests include power electronics circuits, control algorithms, and system modeling for efficient power packet distribution systems.

Dylan Dah-Chuan Lu received his B.S. and Ph.D. degrees from the Hong Kong Polytechnic University, Hong Kong SAR, China, in 1999 and 2004, respectively. In 2003, he joined Power^{e}Lab Ltd. as a Senior Design Engineer where he was responsible for industrial switching power supply projects. He was a full-time faculty member at the University of Sydney from 2006 to 2016, where he now holds an Honorary position. Since July 2016, he has been an Associate Professor at the School of Electrical and Data Engineering, University of Technology Sydney, Sydney, Australia. His current research interest includes efficient and reliable power conversions for renewable sources, energy storage systems, and microgrids. He is a Senior Member of the IEEE and a Member of Engineers Australia. He was a recipient of a Best Paper Award in the category of Emerging Power Electronic Technique at the IEEE PEDS 2015. He is presently serving as an Associate Editor of the IEEE Transactions on Circuits and Systems II and a Subject Editor of the IET Renewable Power Generation.

Ling Qin received his B.S. degree in Electrical Engineering from Southeast University, Nanjing, China, in 1999; and his M.S. and Ph.D. degrees in Electrical Engineering from the Nanjing University of Aeronautics and Astronautics, Nanjing, China, in 2007 and 2017, respectively. From January 2016 to January 2017, he was a Visiting Scholar at the Centre for Future Energy Networks, University of Sydney, Sydney, Australia. He is presently working as an Associate Professor in the Department of Electrical Engineering, Nantong University, Nantong, China. His current research interests include photovoltaic power generation systems, high-frequency dc-dc converters and power electronics system modeling. His work has resulted in more than 50 technical publications and 3 Chinese patents.

Jian Qi received his B.S. (Hons.) degree in Electrical Engineering from the University of Sydney, Sydney, Australia, in 2011, where he is presently working towards his Ph.D. degree in Electrical and Information Engineering. His current research interests include power electronics circuits and control algorithms for efficient and cost-effective battery energy storage systems.